Supporting Information

Effect of ultrasonication on the size distribution and stability of cellulose nanocrystals in suspension: an asymmetrical flow field-flow fractionation study

Christoph Metzger,[1,†] Roland Drexel,[2] Florian Meier,[2] Heiko Briesen[1]

[1]*Technical University of Munich, Germany, TUM School of Life Sciences Weihenstephan, Chair of Process Systems Engineering*

[2]*Postnova Analytics GmbH, Rankinestr. 1, 86899 Landsberg am Lech, Germany*

[†]+49 8161 71-5383

[1]+49 8161 71-4510

[†]christoph.metzger@tum.de

[1]http://svt.wzw.tum.de/

ORCID iDs: Christoph Metzger (0000-0003-1582-8305); Florian Meier (0000-0003-1395-4877); Heiko Briesen (0000-0001-7725-5907)

Operating principle of asymmetrical flow field-flow fractionation

Separation in asymmetrical flow field-flow fractionation (AF4) occurs in a thin, ribbon-like channel where the channel bottom (accumulation wall) is equipped with a semi-permeable ultrafiltration membrane that withholds sample constituents while simultaneously allowing cross flow to pass through. Cross flow is applied perpendicularly to the parabolic channel flow, thereby counteracting the diffusion of sample constituents. In an equilibrium state of forces, smaller sample constituents are located further away from the accumulation wall, compared to larger constituents. They are thus transported in faster streamlines of the channel flow, eluting earlier than larger constituents. Consequently, the retention time of the constituents is directly correlated with their diffusion coefficient, which is convertible to hydrodynamic size using the Stokes-Einstein equation (Schimpf et al. 2000). A further development of AF4 is electrical AF4 (EAF4) where the cross flow is superimposed with an electrical field to facilitate separation based on both size and electrophoretic mobility (**Fig. S1**) (Drexel et al. 2020).

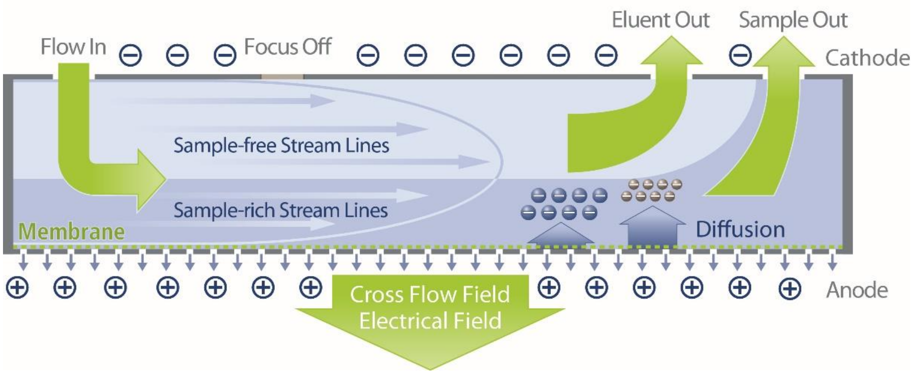

Fig. S1: Longitudinal section of an EAF4 channel (reprinted with permission of Postnova Analytics GmbH)

Literature survey of multi-detector AF4 on cellulose nanocrystal suspensions

Table S1: Summary of studies on multi-detector AF4 for analysis and fractionation of cellulose nanocrystals (CNCs)

Cellulose source	CNC initial state and surface	Detection	Offline validation	Objectives♦	Reference
Microcrystalline cellulose (Avicel), cotton fabric	Never dried, sulfated	MALS, DLS, dRI	TEM	PSD of CNCs – effect of cellulose source and processing; correlated with TEM results	Guan et al. (2012)
Cereal straws (wheat, corn, barley, oat)	Never dried, TEMPO-oxidized	MALS, dRI	DLS	(Qualitative) PSD of polydisperse CNCs	Espinosa et al. (2017)
Microcrystalline cellulose (Avicel)	Never dried, TEMPO-oxidized	MALS, dRI	DLS	Qualitative detection of CNCs in consumer products	Ruiz-Palomero et al. (2017)
Softwood pulp; CNCs supplied by National Research Council, Canada	Spray dried, sulfated, Na^+-exchanged	MALS, DLS, dRI	DLS, TEM	Semi-preparatory CNC fractionation via AF4 for narrow PSDs	Mukherjee and Hackley (2018)
Softwood pulp; CNCs supplied by CelluForce Inc., Windsor, QC, Canada	Spray dried, sulfated, Na^+-exchanged	MALS, DLS, dRI	AFM, DLS, TEM	Fractionation of polydisperse CNCs—facilitated microscopy, correlated PSD, and agglomeration level with TEM results	Chen et al. (2020)

♦Related to purpose of AF4.

Ultrasonication of CNC suspension

$$e_{US} = \frac{ultrasound\ power \cdot treatment\ time}{CNC\ mass} \quad \text{(S1)}$$

Table S2: Process parameters during incremental ultrasonication of CNC suspension

Sample name	CNC-2	CNC-4	CNC-6	CNC-8	CNC-10	CNC-15	CNC-20	CNC-40
Suspension mass /g	243.35	213.32	183.66	153.88	124.05	94.35	64.51	34.70
CNC mass /g	2.43	2.13	1.83	1.54	1.24	0.94	0.64	0.35
Energy input /kJ	4.90	9.13	12.82	15.89	18.36	23.05	26.21	32.81
Treatment time /s	146	274	385	477	551	692	787	985
Targeted e_{US} /kJ g^{-1} CNC	2.00	4.00	6.00	8.00	10.00	15.00	20.00	40.00
Actual e_{US} /kJ g^{-1} CNC	2.01	4.01	6.02	8.02	10.02	14.99	19.91	38.98

Fractionation of CNCs by AF4

Validity of the set-up

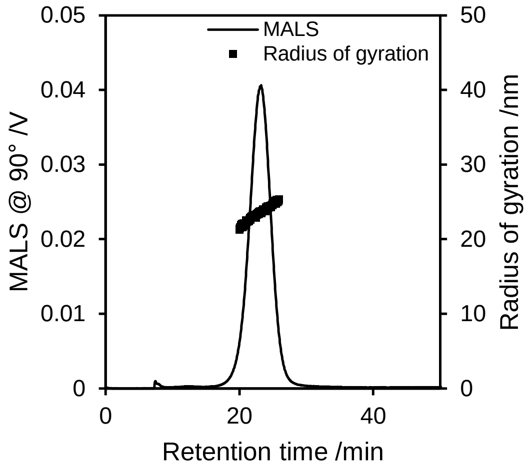

Fig. S2: Fractogram of standard polystyrene beads with a nominal diameter of 60 nm (NIST 2021). r_g was evaluated with the NovaMALS software (Postnova Analytics GmbH 2020)

Our set-up enabled an accurate determination of particles with a $r_g \geq 25$ nm that eluted at net retention times, t_R, $\geq$ 10.6 min (**Fig. S2**). Provided that the applied rod model is valid over the full distribution (Mukherjee and Hackley 2018) and CNCs have a L-d ratio of 5–50 (ISO 2017), a r_g of 25 nm corresponds to particles with a rod length of 87 nm and a minimal L-d ratio of 5 limits them to particle diameters below 17 nm. Notably, single elementary cellulose fibrils of plantal sources have diameters in the range of 3 nm (Kubicki et al. 2018) and reported crystallite dimensions of single CNCs from cotton are in the range from 5–10 nm (Dong et al. 1998, Beck-Candanedo et al. 2005). Accordingly, single CNCs with a length of 87 nm and diameters of 3, 5, or 10 nm have respective L-d ratios of 29, 17, or 9. Likewise, minimal evaluable rod lengths of 95 nm (Guan et al. 2012), 101 nm (Mukherjee and Hackley 2018), and 104 nm (Chen et al. 2020) have been reported for the application of AF4-MALS on colloidal CNCs. Shorter rod lengths determined by AF4-MALS have been reported by Ruiz-Palomero et al. (2017) and Espinosa et al. (2017); however, these values are either not unequivocally attributable to CNCs or methodically not inducible, respectively.

Evolution of maximal multi-angle light scattering intensity

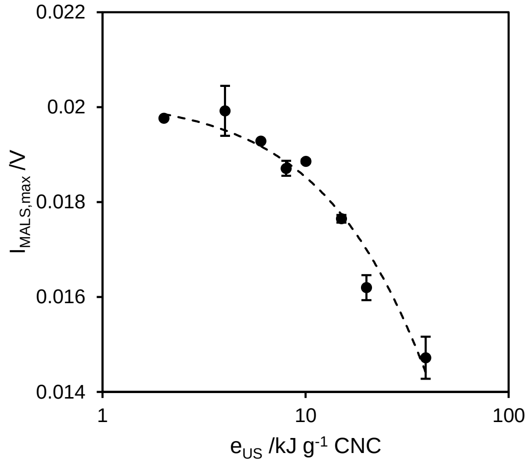

Fig. S3: Maximal intensity of the 90° signal decreases exponentially with increasing ultrasound energy density

Effect of CNC treatment with ion-exchange resins

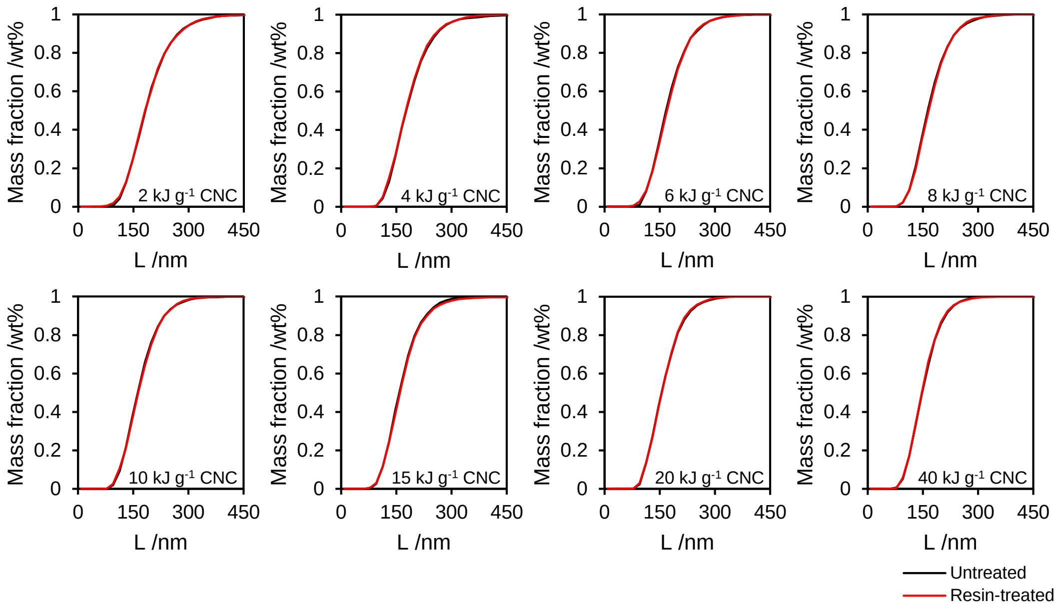

Fig. S4: Particle size distributions of colloidal CNCs before (black) and after (red) treatment with ion-exchange resins at each energy input

Fractograms after CNC conditioning for six months

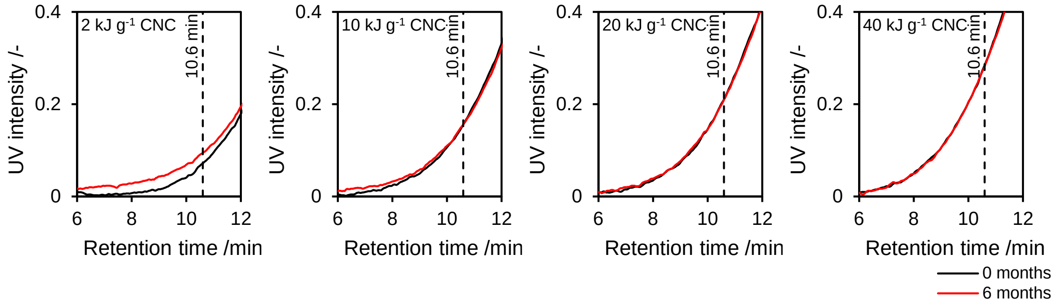

Fig. S5: Normalized UV absorbance signals before (black) and after (red) conditioning of CNC suspensions for six months

References

Beck-Candanedo S, Roman M, Gray DG (2005) Effect of reaction conditions on the properties and behavior of wood cellulose nanocrystal suspensions. Biomacromolecules 6(2):1048–1054. https://doi.org/10.1021/bm049300p

Chen M, Parot J, Mukherjee A, Couillard M, Zou S, Hackley VA, Johnston LJ (2020) Characterization of size and aggregation for cellulose nanocrystal dispersions separated by asymmetrical-flow field-flow fractionation. Cellulose 27(4):2015–2028. https://doi.org/10.1007/s10570-019-02909-9

Dong XM, Revol J-F, Gray DG (1998) Effect of microcrystallite preparation conditions on the formation of colloid crystals of cellulose. Cellulose 5(1):19–32. https://doi.org/10.1023/A:1009260511939

Drexel R, Siupa A, Carnell-Morris P, Carboni M, Sullivan J, Meier F (2020) Fast and Purification-Free Characterization of Bio-Nanoparticles in Biological Media by Electrical Asymmetrical Flow Field-Flow Fractionation Hyphenated with Multi-Angle Light Scattering and Nanoparticle Tracking Analysis Detection. Molecules 25(20). https://doi.org/10.3390/molecules25204703

Espinosa E, Sánchez R, Otero R, Domínguez-Robles J, Rodríguez A (2017) A comparative study of the suitability of different cereal straws for lignocellulose nanofibers isolation. International journal of biological macromolecules 103:990–999. https://doi.org/10.1016/j.ijbiomac.2017.05.156

Guan X, Cueto R, Russo P, Qi Y, Wu Q (2012) Asymmetric flow field-flow fractionation with multiangle light scattering detection for characterization of cellulose nanocrystals. Biomacromolecules 13(9):2671–2679

ISO (2017) ISO/TS 20477:2017 - Nanotechnologies — Standard terms and their definition for cellulose nanomaterial. 2017-10. International Organization for Standardization, Geneva, Switzerland

Kubicki JD, Yang H, Sawada D, O'Neill H, Oehme D, Cosgrove D (2018) The Shape of Native Plant Cellulose Microfibrils. Scientific reports 8(1):13983. https://doi.org/10.1038/s41598-018-32211-w

Mukherjee A, Hackley VA (2018) Separation and characterization of cellulose nanocrystals by multi-detector asymmetrical-flow field-flow fractionation. The Analyst 143(3):731–740. https://doi.org/10.1039/c7an01739a

NIST (2021) SRM 1964 - Polystyrene Spheres (Nominal Diameter 60 nm)

Postnova Analytics GmbH (2020) NovaMALS (1.5.0.8) - https://www.postnova.com/

Ruiz-Palomero C, Laura Soriano M, Valcárcel M (2017) Detection of nanocellulose in commercial products and its size characterization using asymmetric flow field-flow fractionation. Microchimica Acta 184(4):1069–1076. https://doi.org/10.1007/s00604-017-2106-6

Schimpf ME, Caldwell K, Giddings JC (eds) (2000) Field-flow fractionation handbook. Wiley-Interscience, New York, Chichester